Physica B 690 (2024) 416286

Contents lists available at ScienceDirect

Physica B: Condensed Matter

journal homepage: www.elsevier.com/locate/physb

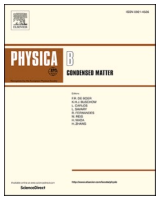

Investigation of AlN-based Schottky type photodetector in visible light detection

A. Kocyigit [a], D.E. Yıldız [b,*], M.O. Erdal [c], A. Tataroglu [d], M. Yıldırım [e]

[a] Department of Electronics and Automation, Vocational High School, Bilecik Şeyh Edebali University, 11000, Bilecik, Turkey
[b] Department of Physics, Faculty of Arts and Sciences, Hitit University, 19030, Corum, Turkey
[c] Meram Vocational School, Necmettin Erbakan University, 42090, Konya, Turkey
[d] Department of Physics, Faculty of Science, Gazi University, 06500, Ankara, Turkey
[e] Department of Biotechnology, Faculty of Science, Selcuk University, 42130, Konya, Turkey

ARTICLE INFO

Keywords:
AlN
Schottky photodetector
Responsivity
Interfacial layer

ABSTRACT

In this study, we fabricated an AlN-based Schottky photodetector by thermal evaporation technique using commercial AlN/n-Si heterojunction which was fabricated by hydride vapor phase epitaxy. Thus, Au/Ti/AlN/n-Si heterostructure was obtained and tested for photodetector applications for various light power densities from 20 mW/cm^2 to 100 mW/cm^2 by *I–V* characteristics. Various parameters of heterostructure were extracted by thermionic emission theory, Norde and Cheung methods to clear the electrical properties of the Au/Ti/AlN/n-Si. Photodetection parameters such as responsivity, photosensitivity, and specific detectivity values were also studied depending on the changing light power density. The Au/Ti/AlN/n-Si photodetector revealed 1.36 A/W responsivity and 7.99×10^9 Jones specific detectivity values. The photoresponse time was investigated by light on-off transient measurements. The Au/Ti/AlN/n-Si photodetector exhibited fast and linear photoresponse to the illumination. The photocapacitance and photoconductance properties of the Au/Ti/AlN/n-Si photodetector were also studied. The results highlighted that Au/Ti/AlN/n-Si photodetector can be a good candidate for fast-response photodetection applications.

1. Introduction

Photodetectors are important parts of the modern world, and research has increased to obtain high-performance photodetectors. They are used for sensing optic electromagnetic radiation by conversion of light into electrical signal, and thus they can be employed in electronic circuits to trigger a system or analyze radiation [1–3]. Photodetectors have a key role in industrial applications ranging from simple light sensing to advanced scientific research [4,5]. They are essential components in various fields including telecommunications, aerospace, medical diagnostics, environmental monitoring, and industrial automation [6]. When incident light hits a photodetector, electron-hole pairs are formed in the interface, and a driven force of the electric field pushes electrons and holes reverse direction towards the outside circuit to obtain electrical current [7]. Photodetectors can be classified as phototransistors, photoresistors, photomultiplers, etc … depending on application areas [8]. They can be sorted into p-n photodetector, avalanche photodetector, pin photodetector, and Schottky photodetector according to their structures [9]. Among them, Schottky photodetector exhibited fast photoresponse and basic structure [10].

Ongoing research and development continue to improve their sensitivity, response time, and reliability, enabling advancements in numerous technological domains [11]. Photodetectors are fabricated by using several active material layers, and researchers have tried to find good-fitting materials for better performance [12–14]. In the case of Schottky photodetectors, various interfacial active layers to catch photons are under investigation [15–17]. Attia et al. used *p*-quaterphenyl film layer as an interfacial layer between Au and p-Si substrate, and they obtained responsivity and specific detectivity values of 0.013 A/W and 2.12×10^8 Jones at the visible region [18]. Dogan et al. used Curcumin pigment to fabricate a Schottky photodetector for UV and visible range detection of light between n-Si and Au metal and they reached 13.19 A/W responsivity and 1.22×10^{11} Jones specific detectivity values [19]. Srivastava et al., deposited pentacene on ITO substrate by spin coating technique to obtain Al/pentacene/ITO Schottky photodetector for UV photodetection, and they attained 1.25×10^{12} Jones specific detectivity

* Corresponding author.
E-mail address: desrayildiz@hitit.edu.tr (D.E. Yıldız).

https://doi.org/10.1016/j.physb.2024.416286
Received 7 March 2024; Received in revised form 3 May 2024; Accepted 7 July 2024
Available online 8 July 2024

and 4.5 A/W responsivity values with very high external quantum efficiencies for UV region [20]. According to these studies, the performance of the Schottky photodetector can be improved by several active materials.

AlN is an interesting material due to having high thermal conductivity, good hardness, high insulation, high dielectric constant of around 8, and well absorption at UV region [21–24]. These behaviors of AlN make it a good candidate for electronic device applications of photodetectors, memory devices, piezoelectric devices, etc.… [25–28]. Some studies used AlN for photodetector applications in metal-semiconductor-metal configuration, but not so many studies employed AlN as an interfacial layer between a metal and semiconductor for Schottky photodetector [29,30]. For that aim, we used commercial AlN/n-Si to fabricate Ti/Au/AlN/n-Si heterostructure for the Schottky photodetector application in this study.

2. Experimental details

Epitaxial growth AlN/n-Si template was commercially bought from MTI Corporation and used directly to fabricate the Schottky photodetector after the cleaning procedure. While the n-Si wafer had (111) orientation, 2-inch diameter, 0.5 mm thicknesses, and 1–10 Ω cm resistivity, the AlN layer was 200 nm thicknesses on n-Si and deposited by hydride vapor phase epitaxy according to the manufacturer. The

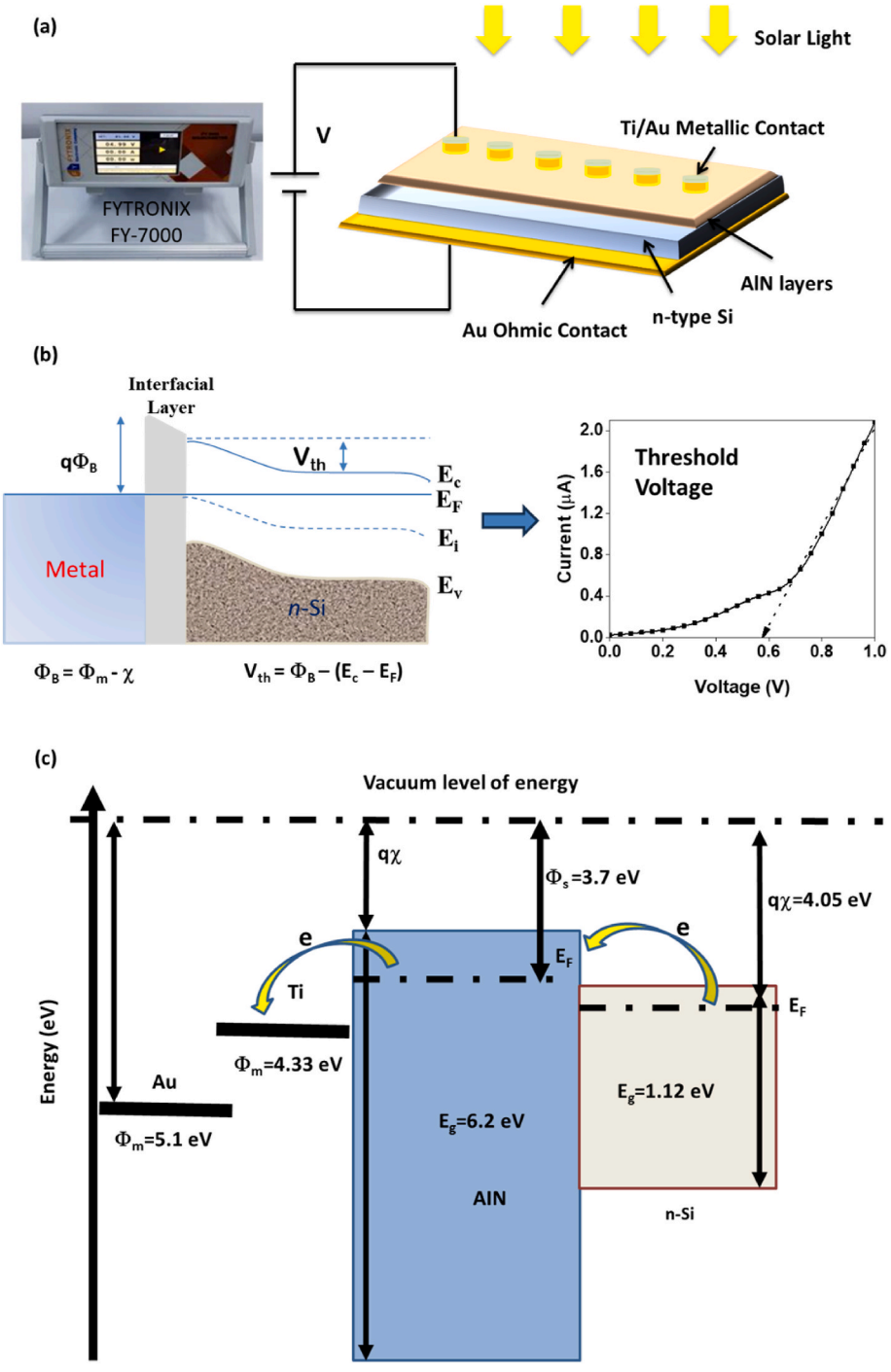

Fig. 1. a) The measurement procedure with schematic structure and b) band diagram of the AlN-based photodetector.

template was divided into 1 × 2 cm^2 slices and then cleaned in an ultrasonic cleaner with 2-propanolinan, acetone, and de-ionized water. The pieces were dried under an N_2 atmosphere and exposed to plasma for 5 min to clean. A 100 nm Au layer was evaporated on the backside of the n-Si pieces by a thermal evaporator at ~10^{-6} Torr, and the pieces were annealed in an N_2 atmosphere at 500 °C only 5 min to accomplish ohmic contact. Au/Ti contact was preferred to obtain low barrier formation since the work function of Au/Ti is smaller than Au or Ti [31–35]. Then, Ti(5 nm)/Au(100) nm metals were evaporated on the AlN surface as 1-diameter circles by a hole array mask. Thus, Ti/Au/AlN/n-Si heterostructure was obtained and tested by *I–V* measurements for dark and different light power densities. Fig. 1a shows the photodetector geometry and measurement system schematically under solar light illumination. The threshold voltage (V_{th}) is a voltage point at forward biases that the diode starts to transmit electrical current immediately. Generally, lower V_{th} is desired, and its value is about 0.2–0.3 V for Schottky diodes. Fig. 1b shows a schematic illustration of the V_{th} and determination graphs of the AlN-based photodetector. The energy-band diagram for Au/Ti/AIN/n-Si photodiode is given in Fig. 1c. As seen in this figure, the work function ($_M$) of Ti and Au is 4.33 and 5.1 eV, respectively. The energy band gap of AlN and n-Si is 6.2 and ~1.12 eV, respectively. Also, the electron affinity (χ_s) of n-Si is ~4.05 eV.

SEM image of the AlN/n-Si was taken by QUANTA 400F Field Emission SEM. Current-transient and current-voltage results were collected by the FYTRONIX FY-7000 Solar Simulator under dark and several light power densities. Transient capacitance and conductance measurements depending on various light power densities were obtained by ST2826/A High Frequency LCR Meter under a solar simulator.

3. Results and discussion

Surface morphology images of the AlN template were studied by field emission SEM for various magnifications to check the suitability of a photodetector. Fig. 2a–d shows SEM images of the AlN/n-Si template for increasing magnifications from 1kx to 30 kx. Structures of the AlN exhibited porous surfaces with some holes with homogenously distributed on the surface. We think that the porous structure of AIN as an insulator can improve the performance of the photodetector [36].

A device's *I–V* characteristics give information about the passing current through the device by applied external voltage. In the case of Schottky photodetector as well as diodes, the current passes after a threshold value at forward biases, but it is stopped at reverse biases. Fig. 3a shows *I–V* characteristics of the Au/Ti/AlN/n-Si heterostructure for several light power densities. The threshold voltage (V_{th}) values were determined by a close look at forward bias *I–V* characteristics (inset) depending on the light power density and given in Fig. 3b. The Au/Ti/AlN/n-Si heterostructure reveals an increase in the current at the reverse and forward biases, and it can be used as photodetector applications. The reason for the current increase at reverse biases by increasing voltage can depend on the defect levels at the interface with the AlN interlayer [37]. V_{th} values decreased from 0.58 V to 0.44 V by increasing light power density because of increasing current depending on light power. This result confirms that the Au/Ti/AlN/n-Si heterostructure is

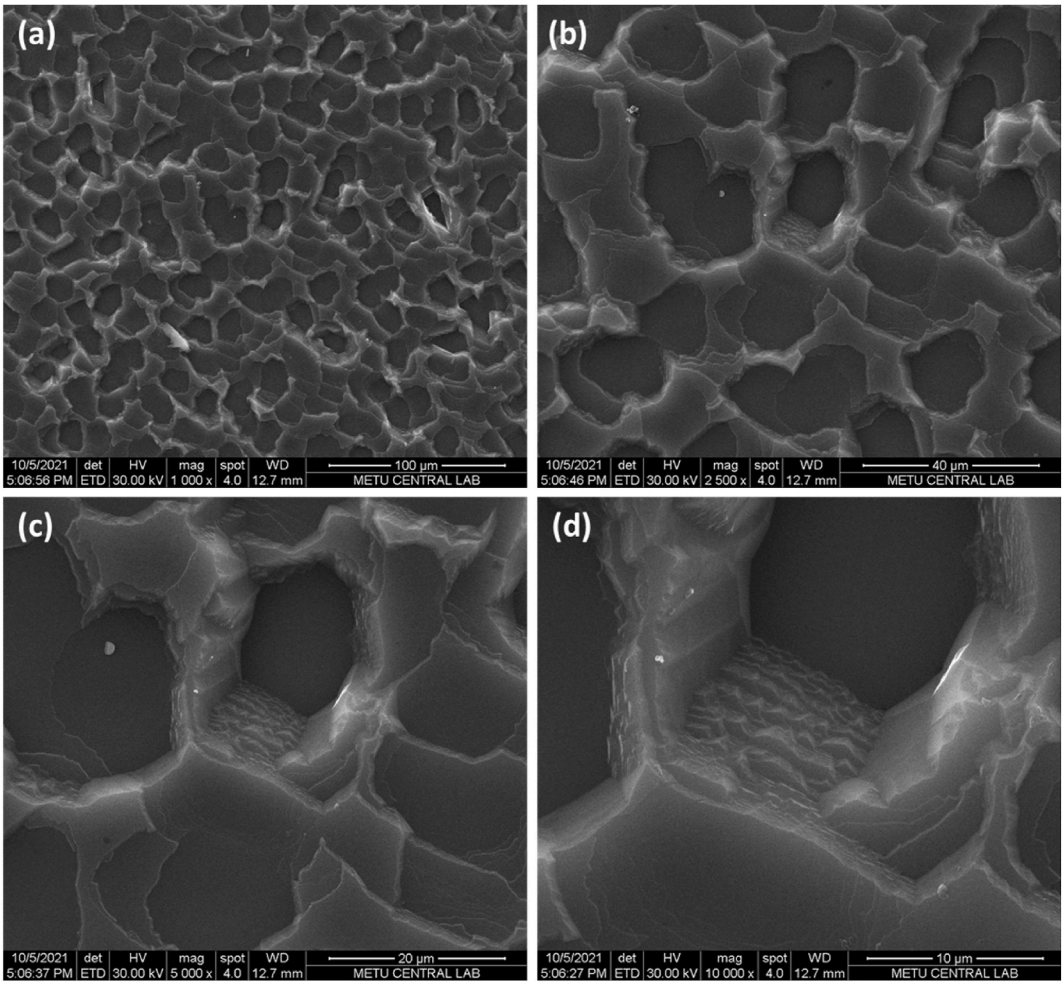

Fig. 2. SEM images of the AlN interlayers for various magnification.

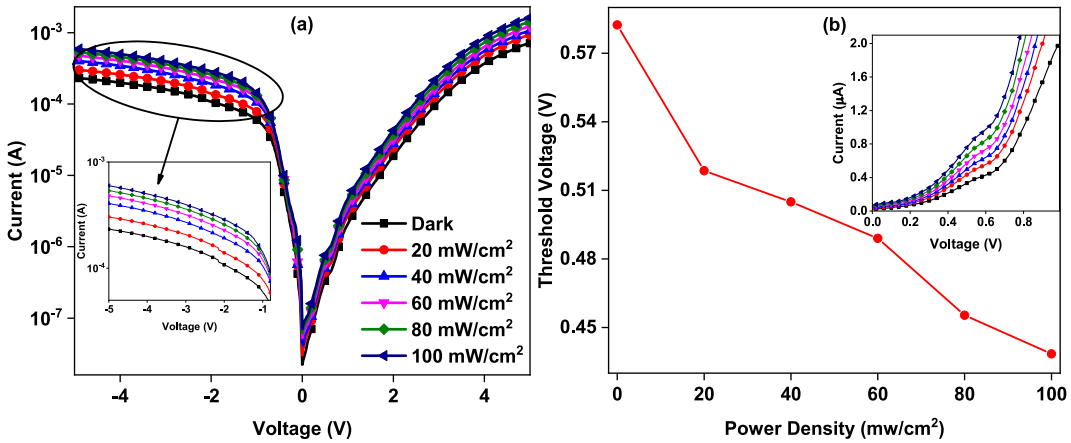

Fig. 3. a) *I–V* characteristics and b) threshold voltage changes of the Au/Ti/AlN/n-Si photodetector for changing light power density.

sensitive to light illumination.

Several heterostructure parameters of ideality factor (n), series resistance (R_s), shunt resistance (R_{sh}), and barrier height (Φ_b) can be determined to understand the electrical behaviors of the Au/Ti/AlN/n-Si heterostructure. Thermionic emission theory is employed to figure out some of these parameters, and a detailed explanation of the method can be discovered everywhere [38–46]. The n and Φ_b values have been determined for various light power densities and given in Fig. 4a. While the Φ_b values increased with decreasing light power density, n values have a reverse profile. These results highlight that the Au/Ti/AlN/n-Si heterostructure has a response to changing light power density, and light causes easily electron-hole pairs in the interface of the heterostructure and change parameters. While the Φ_b values are in good agreement with many Schottky photodetectors, the n values are much higher than unity or their ideal values [47]. These high ideality factor values can be dependent on the interfacial AlN layer, interface states, or series resistance effect [48]. Junction resistance (R_j) of the Au/Ti/AlN/n-Si heterostructure can be obtained by dV/dI formula from *I–V* characteristics to determine R_{sh} and R_s values from reverse and forward bias regions [49]. R_j-V plots of the Au/Ti/AlN/n-Si heterostructure have been displayed in Fig. 4b depending on the changing light power density. Both the R_{sh} and R_s values have a decreasing profile with increasing light power density because of the increasing current level. The R_{sh} and R_s values were determined as around 10^4 Ω and 10^3 Ω levels. The changing of the R_j values with light power density implies that the Au/Ti/AlN/n-Si heterostructure has a response to illumination.

To confirm the above parameters, the Norde and Cheung methods can be employed since the Norde method helps to calculate R_s and Φ_b values from the Norde function, and the Cheung method provides to determine n, Φ_b, and R_s values from the $dV/d(\ln I)$ and $H(I)$ functions. The details about the calculation of these parameters can be found in the literature [50,51]. The Norde function and Cheung's functions of $dV/d(\ln I)$ and $H(I)$ have been calculated and plotted in Fig. 5a and b for dependent voltage and current, respectively in the case of dark conditions. While the Norde function exhibits the Norde plot, Cehung's functions display an almost linear profile. While the R_s values were determined as 786 kΩ and 65.9 kΩ, the Φ_b values were obtained as 0.73 eV and 0.72 eV from the Norde and Cheung methods, respectively. The n value was calculated as 7.41 which was close to n of thermionic emission theory. These all values are in good agreement with each other by small differences in approximations [52].

The current transient (*I-t*) measurements provide information about the photodetector response to illumination. Fig. 6a shows *I-t* plots Au/Ti/AlN/n-Si photodetector for increasing light power density. When the light is on, the current immediately increases to change all light power intensities. The Au/Ti/AlN/n-Si photodetector has an almost linear current increase for increasing light power intensity. Fig. 6b indicates a close look at the *I-t* plots Au/Ti/AlN/n-Si for showing rise and fall times. Both rise and fall times were determined as 400 ms from 10 % to 90 % current values.

The detector parameters of photosensitivity (K), photocurrent (I_p), specific detectivity (D^*), and responsivity (R) values can be calculated by following formulas [53,54]:

$$I_p = I_{light} - I_{dark} \tag{1}$$

$$K = \frac{I_p}{I_{dark}} \tag{2}$$

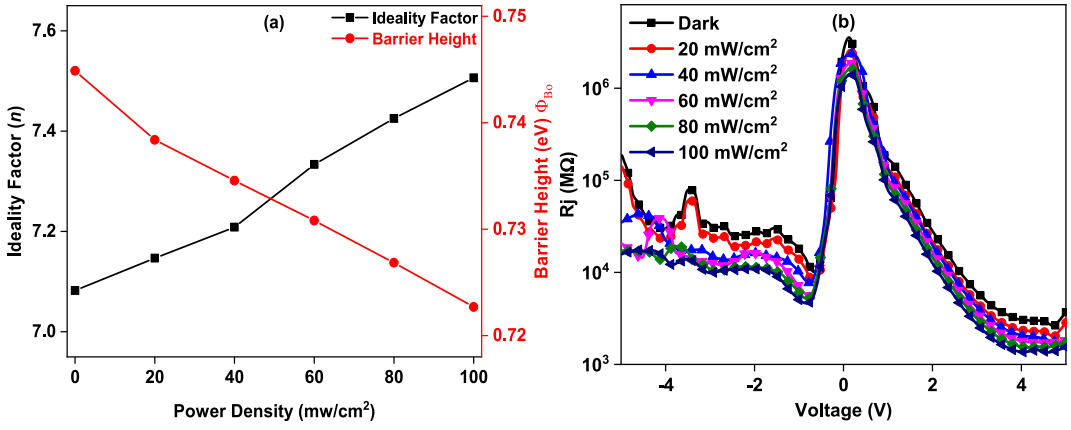

Fig. 4. a) n - Φ_b profiles and b) R_j-V characteristics of the Au/Ti/AlN/n-Si photodetector for changing light power density.

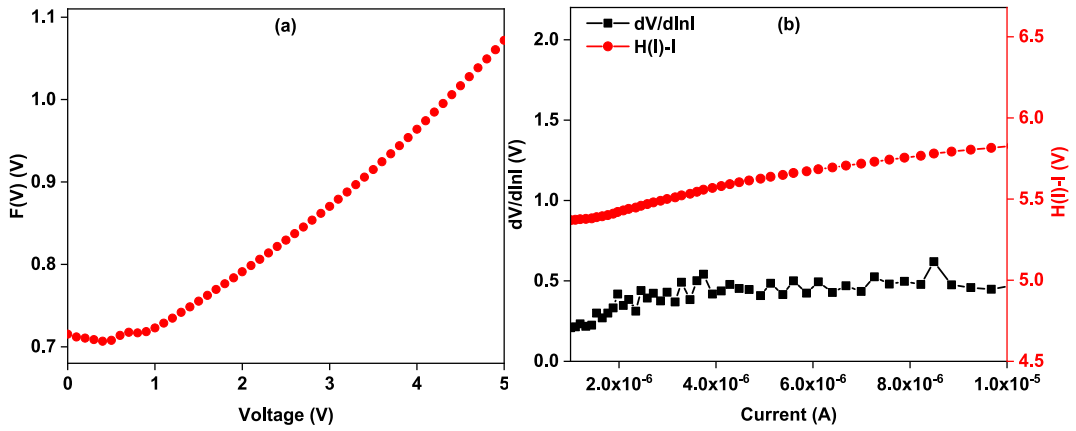

Fig. 5. *F(V)–V* plots a) and b) Cheung plots of Au/Ti/AlN/n-Si photodetector for dark condition.

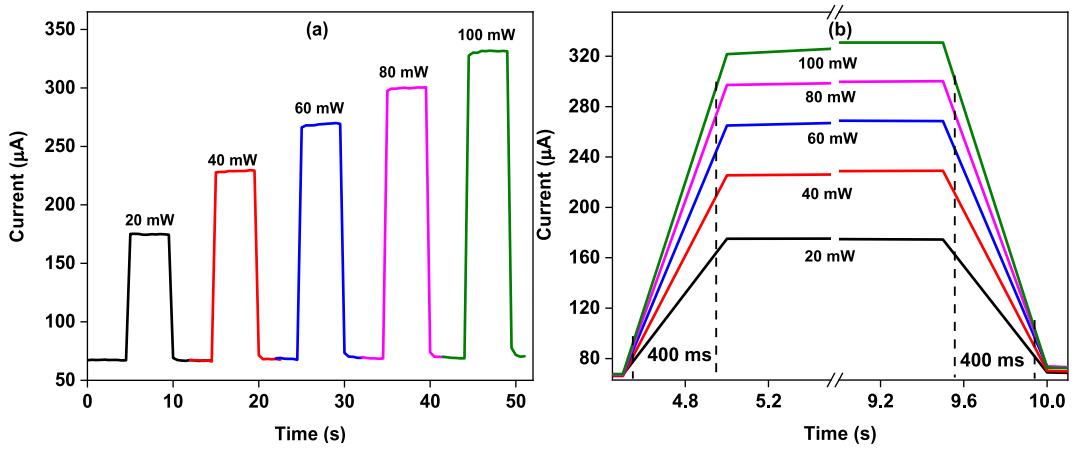

Fig. 6. a) *I-t* plots Au/Ti/AlN/n-Si photodetector and b) close looks of *I-t* plots for determining the rise and fall times.

$$R = \frac{I_p}{PA} \tag{3}$$

$$D^* = R\sqrt{\frac{A}{2qI_{dark}}} \tag{4}$$

While the *A* represents the effective detector area, the *P* and q show light power density and charge of electrons. The photoconduction mechanism of a photodetector can be determined by the next expression:

$$I_p = \alpha P^m \tag{5}$$

where α is a constant, and *m* represents the linearity ratio between light power density and photocurrent. The *m* value can be obtained from the slope of Log I_p versus Log *p*. If the *m* values are in between 0.5 and 1.0, the localized trap levels have continued distribution. On the other hand, the transmission of current can be controlled by localized trap states [55]. Fig. 7a shows Log I_p versus Log *p* plots of the Au/Ti/AlN/n-Si photodetector, and confirms localized trap leveled control of the current transmission. Fig. 7b, c, and 7d show light power density-dependent *K*, *R*, and *D** changes. While the photosensitivity values almost linearly increased, responsivity and specific detectivity values exhibited the same profile of decreasing. The photocurrent, photosensitivity, responsivity, and specific detectivity values are listed in Table 1 for several light power densities. The maximum responsivity and specific detectivity values were determined as 1.36 A/W and 7.99 × 10^9 Jones for 20 mW/cm^2 power density. The decrease in the responsivity and specific detectivity values can be attributed to the gradual photosensing saturation of the Au/Ti/AlN/n-Si photodetector [56]. The obtained responsivity and specific detectivity values are in good agreement with Schottky photodetectors [57–59].

Transient capacitance and conductance values give information about the photoconduction mechanism of a photodetector [60]. Fig. 8a and b exhibit capacitance and conductance changes of the Au/Ti/AlN/n-Si photodetector depending on increasing light power intensity for 10 kHz frequency. Both the capacitance and conductance values immediately increased by increasing light power density. These results confirmed that Au/Ti/AlN/n-Si photodetector exhibited photoconduction mechanism by photogenerated charge carriers [61].

4. Conclusion

Au/Ti/AlN/n-Si Schottky photodetector was fabricated by thermal evaporation technique with AlN/n-Si commercial template. The SEM image of the AlN layer revealed a porous structure. The obtained photodetector was characterized by *I–V* characteristics for various light power densities. The heterojunction parameters of series resistance, ideality factor, and barrier height values were extracted and discussed depending on increasing light power density. The photodetection parameters such as photocurrent, photosensitivity, responsivity, and specific detectivity values were obtained and discussed depending on changing light power density. The Au/Ti/AlN/n-Si photodetector revealed 1.36 A/W responsivity and 7.99 × 10^9 Jones specific detectivity values. Photoresponse time was investigated by light on-off transient measurements and obtained 400 ms rise and fall times. The photocapacitance and photoconductance properties of the Au/Ti/AlN/

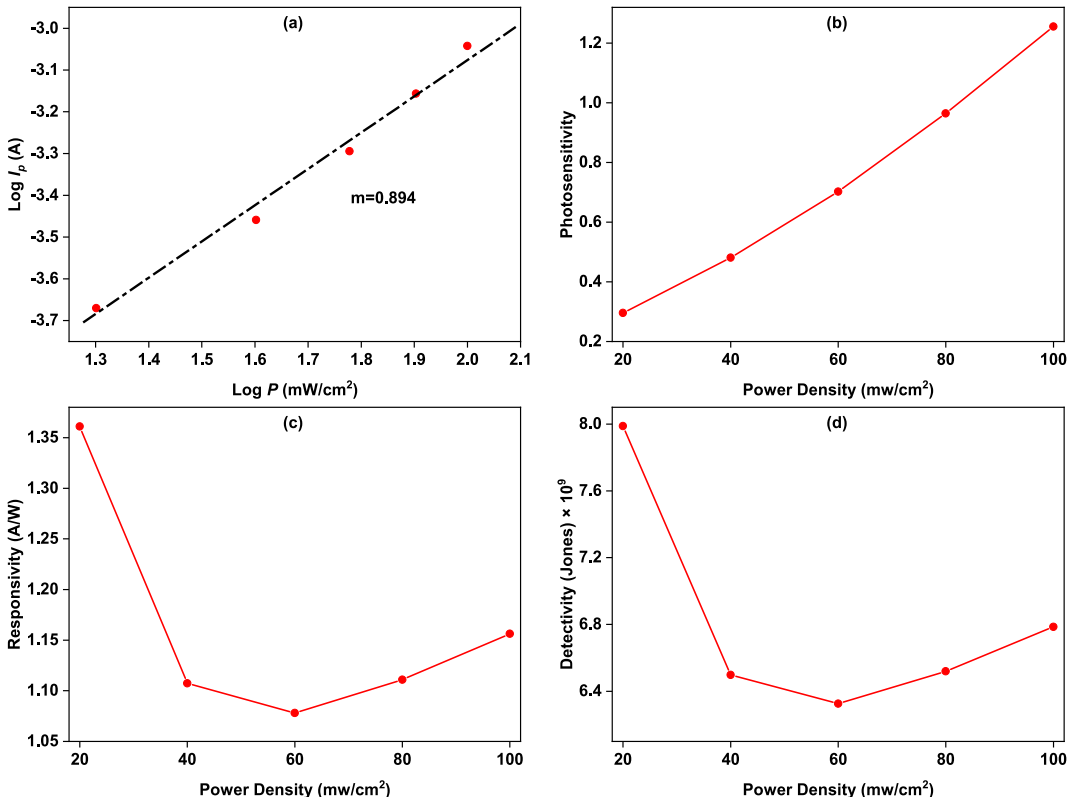

Fig. 7. a) Photocurrent, b) photosensitivity changes, c) responsivity and detectivity of the Au/Ti/AlN/n-Si photodetector for changing light power.

Table 1
The photodetection parameters of the Au/Ti/AlN/n-Si photodetector.

Power density (mW/cm^2)	Photocurrent (A)	Photosensitivity –	Responsivity (A/W)	Specific detectivity (Jones)
20	2.14×10^{-4}	0.296	1.36	7.99×10^{9}
40	3.48×10^{-4}	0.481	1.11	6.50×10^{9}
60	5.08×10^{-4}	0.702	1.08	6.33×10^{9}
80	6.98×10^{-4}	0.965	1.11	6.52×10^{9}
100	9.08×10^{-4}	1.255	1.16	6.79×10^{9}

n-Si revealed that the photodetector exhibited photocoduction mechanism due to photogenerated charges.

CRediT authorship contribution statement

A. Kocyigit: Writing – review & editing, Methodology, Investigation. **D.E. Yıldız:** Writing – review & editing, Writing – original draft, Methodology, Investigation, Formal analysis, Data curation, Conceptualization. **M.O. Erdal:** Methodology, Investigation, Formal analysis, Conceptualization. **A. Tataroglu:** Methodology, Investigation, Formal analysis. **M. Yıldırım:** Writing – original draft, Methodology, Investigation, Data curation, Conceptualization.

Declaration of competing interest

The authors declare that they have no known competing financial

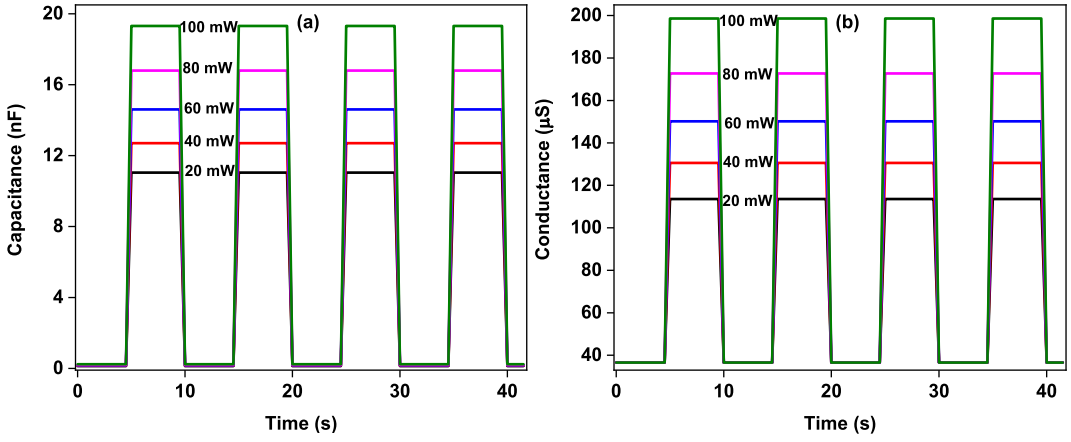

Fig. 8. a) Photocapacitance and b) photoconductance changes of Au/Ti/AlN/n-Si photodetector for changing light power.

interests or personal relationships that could have appeared to influence the work reported in this paper.

Data availability

Data will be made available on request.

References

[1] B. Ezhilmaran, A. Patra, S. Benny, S.M. R, A.V. V, S.V. Bhat, C.S. Rout, Recent developments in the photodetector applications of schottky diodes based on 2D materials, J. Mater. Chem. C 9 (2021) 6122–6150, https://doi.org/10.1039/d1tc00949d.

[2] S.K. Pradhan, S. Sahu, P.K. Das, Photodetector based Auto trigger system using kalman filter, in: 2021 2nd Int. Conf. Range Technol., IEEE, 2021, pp. 1–4, https://doi.org/10.1109/ICORT52730.2021.9581837.

[3] T. Yang, F. Li, R. Zheng, Recent advances in radiation detection technologies enabled by metal-halide perovskites, Mater. Adv. 2 (2021) 6744–6767, https://doi.org/10.1039/D1MA00569C.

[4] D. Kong, Y. Zhou, J. Chai, S. Chen, L. Chen, L. Li, T. Lin, W. Wang, G. Li, Recent progress in InGaN-based photodetectors for visible light communication, J. Mater. Chem. C 10 (2022) 14080–14090, https://doi.org/10.1039/D2TC02122F.

[5] Y. Ma, X. Xie, W. Yang, Z. Yu, X. Sun, Y. Zhang, X. Yang, H. Kimura, C. Hou, Z. Guo, W. Du, Recent advances in transition metal oxides with different dimensions as electrodes for high-performance supercapacitors, Adv. Compos. Hybrid Mater. 4 (2021) 906–924, https://doi.org/10.1007/s42114-021-00358-2.

[6] H. Ren, J. Chen, Y. Li, J. Tang, Recent progress in organic photodetectors and their applications, Adv. Sci. 8 (2021), https://doi.org/10.1002/advs.202002418.

[7] K. Wu, X. Liao, M.A. Iqbal, Y.-J. Zeng, Research progress on topological material-based photodetectors, Mater. Adv. 4 (2023) 5018–5032, https://doi.org/10.1039/D3MA00452J.

[8] D.A. Ross, Solid state photodetectors — the photodiode and phototransistor, in: Optoelectron. Devices Opt. Imaging Tech., Macmillan Education UK, London, 1979, pp. 31–47, https://doi.org/10.1007/978-1-349-16219-2_4.

[9] Y. Wei, C. Lan, S. Zhou, C. Li, Recent advances in photodetectors based on two-dimensional material/Si heterojunctions, Appl. Sci. 13 (2023) 11037, https://doi.org/10.3390/app131911037.

[10] R.S. Quimby, Photodiode detectors, in: Photonics and Lasers, John Wiley & Sons, Inc., Hoboken, NJ, USA, 2006, pp. 249–279, https://doi.org/10.1002/0471791598.ch14.

[11] X. Li, X. Wang, Y. Ma, W. Deng, Y. Wu, J. Li, K. Li, Y. Zhang, Recent progress in functional two-dimensional photovoltaic photodetectors and related emerging applications, J. Mater. Chem. A. 11 (2023) 11548–11571, https://doi.org/10.1039/D3TA00950E.

[12] M. Malik, M.A. Iqbal, J.R. Choi, P.V. Pham, 2D materials for efficient photodetection: Overview, mechanisms, performance and UV-IR range applications, Front. Chem. 10 (2022) 488, https://doi.org/10.3389/fchem.2022.905404.

[13] C. Liu, J. Guo, L. Yu, J. Li, M. Zhang, H. Li, Y. Shi, D. Dai, Silicon/2D-material photodetectors: from near-infrared to mid-infrared, Light Sci. Appl. 10 (2021) 1–21, https://doi.org/10.1038/s41377-021-00551-4.

[14] C. Yang, G. Wang, M. Liu, F. Yao, H. Li, Mechanism, material, design, and implementation principle of two-dimensional material photodetectors, Nanomaterials 11 (2021) 2688, https://doi.org/10.3390/nano11102688.

[15] M. Mohammed, Z. Li, J. Cui, T. Chen, Acid-doped multi-wall carbon nanotube/n-Si heterojunctions for enhanced light harvesting, Sol. Energy 106 (2014) 171–176, https://doi.org/10.1016/j.solener.2014.03.014.

[16] A. Kocyigit, M. Yıldırım, A. Sarılmaz, F. Ozel, The Au/Cu2WSe4/p-Si photodiode: electrical and morphological characterization, J. Alloys Compd. 780 (2019) 186–192, https://doi.org/10.1016/j.jallcom.2018.11.372.

[17] A. Kocyigit, M. Yılmaz, Ü. İncekara, Y. Şahin, Ş. Aydoğan, The light detection performance of the congo red dye in a schottky type photodiode, Chem. Phys. Lett. 800 (2022) 139673, https://doi.org/10.1016/j.cplett.2022.139673.

[18] A.A. Attia, M.M. Saadeldin, H.S. Soliman, A.-S. Gadallah, K. Sawaby, Structural and optical properties of p-quaterphenyl thin films and application in organic/inorganic photodiodes, Opt. Mater. 62 (2016) 711–716, https://doi.org/10.1016/j.optmat.2016.10.046.

[19] H.O. Dogan, F. Yıldırım, Z. Orhan, A. Ben Ahmed, M. Benhaliliba, Ş. Aydoğan, Numerical evaluations of curcumin organic molecule and an experimental study on hybrid photodetector performance in visible and UV regions, Org. Electron. 124 (2024) 106946, https://doi.org/10.1016/j.orgel.2023.106946.

[20] A. Srivastava, S. Jit, S. Tripathi, High-performance solution-processed pentacene/Al Schottky ultraviolet photodiode with pseudo photovoltaic effect, IEEE Trans. Electron Devices 67 (2020) 4300–4307, https://doi.org/10.1109/TED.2020.3013557.

[21] N. Matsunami, H. Kakiuchida, M. Sataka, S. Okayasu, XRD characterization of AlN thin films prepared by reactive RF-sputter deposition, Adv. Mater. Phys. Chem. 3 (2013) 101–107, https://doi.org/10.4236/ampc.2013.31A012.

[22] J.A. Brant, C.D. Brunetta, J.A. Aitken, Chalcogenides and nonoxides, in: Compr. Inorg. Chem., vol. II, Elsevier, 2013, pp. 213–283, https://doi.org/10.1016/B978-0-08-097774-4.00510-6.

[23] N. Ben Hassine, D. Mercier, P. Renaux, G. Parat, S. Basrour, P. Waltz, C. Chappaz, P. Ancey, S. Blonkowski, Dielectrical properties of metal-insulator-metal aluminum nitride structures: measurement and modeling, J. Appl. Phys. 105 (2009), https://doi.org/10.1063/1.3081977.

[24] S. Maouhoub, Y. Aoura, A. Mir, FEM simulation of AlN thin layers on diamond substrates for high frequency SAW devices, Diam. Relat. Mater. 62 (2016) 7–13, https://doi.org/10.1016/j.diamond.2015.12.004.

[25] X. Liu, J. Luo, Y. Lin, Z. Lin, X. Liu, J. He, W. Yu, Q. Liu, T. Wei, J. Yang, W. Zhang, J. Guo, High-performance photodetectors using a 2D MoS 2/3D-AlN structure, ACS Appl. Electron. Mater. 3 (2021) 5415–5422, https://doi.org/10.1021/acsaelm.1c00882.

[26] M. Khaouani, A. Hamdoune, H. Bencherif, Z. Kourdi, L. Dehimi, An ultra-sensitive AlGaN/AlN/GaN/AlGaN photodetector: proposal and investigation, Optik 217 (2020) 164797, https://doi.org/10.1016/j.ijleo.2020.164797.

[27] S.T. Haider, M.A. Shah, D.-G. Lee, S. Hur, A review of the recent applications of aluminum nitride-based piezoelectric devices, IEEE Access 11 (2023) 58779–58795, https://doi.org/10.1109/ACCESS.2023.3276716.

[28] N. Ben Hassine, D. Mercier, P. Renaux, G. Parat, S. Basrour, P. Waltz, C. Chappaz, P. Ancey, S. Blonkowski, Dielectrical properties of metal-insulator-metal aluminum nitride structures: measurement and modeling, J. Appl. Phys. 105 (2009), https://doi.org/10.1063/1.3081977.

[29] J. Li, Z.Y. Fan, R. Dahal, M.L. Nakarmi, J.Y. Lin, H.X. Jiang, 200 nm deep ultraviolet photodetectors based on AlN, Appl. Phys. Lett. 89 (2006), https://doi.org/10.1063/1.2397021.

[30] A. BenMoussa, J.F. Hochedez, R. Dahal, J. Li, J.Y. Lin, H.X. Jiang, A. Soltani, J.-C. De Jaeger, U. Kroth, M. Richter, Characterization of AlN metal-semiconductor-metal diodes in the spectral range of 44–360nm: photoemission assessments, Appl. Phys. Lett. 92 (2008), https://doi.org/10.1063/1.2834701.

[31] A. Turut, D.E. Yıldız, A. Karabulut, I. Orak, Electrical characteristics of atomic layer deposited Au/Ti/HfO2/n-GaAs MIS diodes in the wide temperature range, J. Mater. Sci. Mater. Electron. 31 (2020) 7839–7849, https://doi.org/10.1007/s10854-020-03322-w.

[32] D.E. Yıldız, A. Tataroglu, Analysis of dielectric, impedance and electrical properties of interfacial layer: AlN, J. Mater. Sci. Mater. Electron. 34 (2023) 1057, https://doi.org/10.1007/s10854-023-10235-x.

[33] I.B. Chistokhin, M.S. Aksenov, N.A. Valisheva, D.V. Dmitriev, A.P. Kovchavtsev, A. K. Gutakovskii, I.P. Prosvirin, K.S. Zhuravlev, Barrier characteristics and interface properties of Au/Ti/n-InAlAs Schottky contacts, Mater. Sci. Semicond. Process. 74 (2018) 193–198, https://doi.org/10.1016/j.mssp.2017.10.014.

[34] V.R. Reddy, Y.M. Reddy, R. Padmasuvarna, T.L. Narasappa, Ru/Ti Schottky contacts on N-type in-P (100): temperature dependence of current-voltage (I-V) characteristics, Procedia Mater. Sci. 10 (2015) 666–672, https://doi.org/10.1016/j.mspro.2015.06.060.

[35] N. Biyikli, A. Karabulut, H. Efeolu, B. Guzeldir, A. Turut, Electrical characteristics of Au/Ti/n-GaAs contacts over a wide measurement temperature range, Phys. Scr. 89 (2014) 095804, https://doi.org/10.1088/0031-8949/89/9/095804.

[36] L. Zhao, C. Liu, K. Wang, Progress of GaN-based optoelectronic devices integrated with optical resonances, Small 18 (2022), https://doi.org/10.1002/smll.202106757.

[37] T. Hamachi, T. Tohei, Y. Hayashi, M. Imanishi, S. Usami, Y. Mori, A. Sakai, Comprehensive analysis of current leakage at individual screw and mixed threading dislocations in freestanding GaN substrates, Sci. Rep. 13 (2023) 2436, https://doi.org/10.1038/s41598-023-29458-3.

[38] İ. Uzun, L. Bilal Taşyürek, İ. Orak, M. Karakaplan, Evaluation of synthesized new cellulose derivatives to make diodes and investigation of electrical and photoelectrical characteristics of these diodes, Mater. Sci. Eng. B. 300 (2024) 117111, https://doi.org/10.1016/j.mseb.2023.117111.

[39] K. Mensah-Darkwa, R.O. Ocaya, A.G. Al-Sehemi, D. Yeboah, A. Dere, A.A. Al-Ghamdi, R.K. Gupta, F. Yakuphanoğlu, Optoelectronic enhancement of ZnO/p-Si Schottky barrier photodiodes by (Sn,Ti) co-doping, Phys. B Condens. Matter 667 (2023) 415155, https://doi.org/10.1016/j.physb.2023.415155.

[40] G. Güler, Ö. Güllü, Ş. Karataş, Ö.F. Bakkaloğlu, Analysis of the series resistance and interface state densities in metal semiconductor structures, J. Phys. Conf. Ser. 153 (2009) 012054, https://doi.org/10.1088/1742-6596/153/1/012054.

[41] Ş. Karataş, M. Çakar, Temperature dependence of the electrical and interface states of the Sn/Rhodamine-101/p-Si Schottky structures, Synth. Met. 159 (2009) 347–351, https://doi.org/10.1016/j.synthmet.2008.11.025.

[42] İ. Orak, A. Kocyiğit, Ş. Karataş, The analysis of the electrical and photovoltaic properties of Cr/p-Si structures using current-voltage measurements, Silicon 10 (2018) 2109–2116, https://doi.org/10.1007/s12633-017-9731-x.

[43] H. Özerli, A. Bekereci, A. Türüt, Ş. Karataş, Electrical and photovoltaic properties of Ag/p-Si structure with GO doped NiO interlayer in dark and under light illumination, J. Alloys Compd. 718 (2017) 75–84, https://doi.org/10.1016/j.jallcom.2017.05.121.

[44] M. Çavaş, F. Yakuphanoğlu, Ş. Karataş, The electrical properties of photodiodes based on nanostructure gallium doped cadmium oxide/p-type silicon junctions, Indian J. Phys. 91 (2017) 413–420, https://doi.org/10.1007/s12648-016-0952-4.

[45] H. Seymen, N. Berk, İ. Orak, Ş. Karataş, Effect of illumination intensity on the electrical characteristics of Au//SiO2/n-type Si structures with GO and P3C4MT interface layer, J. Mater. Sci. Mater. Electron. 33 (2022) 19656–19666, https://doi.org/10.1007/s10854-022-08801-w.

[46] Ş. Karataş, N. Berk, Performance of the illumination dependent electrical and photodiode characteristic of the Al/(GO:PTCDA)/p-Si structures, Opt. Mater. 126 (2022) 112231, https://doi.org/10.1016/j.optmat.2022.112231.

[47] Z. Huang, Y. Mao, G. Lin, X. Yi, A. Chang, C. Li, S. Chen, W. Huang, J. Wang, Low dark current broadband 360-1650 nm ITO/Ag/n-Si Schottky photodetectors, Opt Express 26 (2018) 5827, https://doi.org/10.1364/OE.26.005827.

[48] I. Orak, A. Kocyigit, A. Turut, The surface morphology properties and respond illumination impact of ZnO/n-Si photodiode by prepared atomic layer deposition technique, J. Alloys Compd. 691 (2017) 873–879, https://doi.org/10.1016/j.jallcom.2016.08.295.
[49] S. Demirezen, A. Dere, H.G. Çetinkaya, A.G. Al-Sehemi, A.A. Al-Ghamdi, F. Yakuphanoglu, Hybrid photonic device based on Graphene Oxide (GO) doped P3HT-PCBM/p-Silicon for photonic applications, Phys. Scr. 98 (2023) 115916, https://doi.org/10.1088/1402-4896/acfce2.
[50] A. Tataroğlu, Ş. Altındal, Y. Azizian-Kalandaragh, Comparison of electrical properties of MS and MPS type diode in respect of (In2O3-PVP) interlayer, Phys. B Condens. Matter 576 (2020) 411733, https://doi.org/10.1016/j.physb.2019.411733.
[51] A.K. Bilgili, T. Güzel, M. Özer, Current-voltage characteristics of Ag/TiO2/n-InP/Au Schottky barrier diodes, J. Appl. Phys. 125 (2019) 035704, https://doi.org/10.1063/1.5064637.
[52] Z. Orhan, M. Yilmaz, S. Aydogan, M. Taskin, U. Incekara, Improving light-sensing behavior of Cu/n-Si photodiode with Human Serum Albumin: microelectronic and dielectric characterization, Optik 241 (2021) 167069, https://doi.org/10.1016/j.ijleo.2021.167069.
[53] D.E. Yıldız, A. Kocyigit, M. Yıldırım, Comparison of Al/TiO2/p-Si and Al/ZnO/p-Si photodetectors, Opt. Mater. 145 (2023) 114371, https://doi.org/10.1016/j.optmat.2023.114371.
[54] Z. Bielecki, K. Achtenberg, M. Kopytko, J. Mikołajczyk, J. Wojtas, A. Rogalski, Review of photodetectors characterization methods, Bull. Polish Acad. Sci. Tech. Sci. 70 (2022), https://doi.org/10.24425/BPASTS.2022.140534.
[55] Ö. Sevgili, F. Lafzi, A. Karabulut, İ. Orak, S. Bayındır, The synthesis of new bola-amphiphile TPEs and the comparison of current transformer mechanism and structural properties for Al/Bis(HCTA)-TPE/p-Si and Al/Bis(HCOA)-TPE/p-Si heterojunctions, Compos. Part B Eng. 172 (2019) 226–233, https://doi.org/10.1016/j.compositesb.2019.05.020.
[56] L. Tao, S. Li, B. Yao, M. Xia, W. Gao, Y. Yang, X. Wang, N. Huo, Raman anisotropy and polarization-sensitive photodetection in 2D Bi2O2Se–WSe2 heterostructure, ACS Omega 6 (2021) 34763–34770, https://doi.org/10.1021/acsomega.1c05246.
[57] Z. Orhan, H. Öztürk Doğan, Ş. Aydoğan, S. Sarıtaş, B. Kurt Urhan, Hydrogen gas sensing and photodetector applications on electrofabricated Pd@CuCo2O4 nanostructures, Ceram. Int. 50 (2024) 8472–8479, https://doi.org/10.1016/j.ceramint.2023.12.182.
[58] Y. Tang, J. Chen, High responsivity of Gr/n-Si Schottky junction near-infrared photodetector, Superlattices Microstruct 150 (2021) 106803, https://doi.org/10.1016/j.spmi.2021.106803.
[59] C. Yang, S. Qin, Y. Zuo, Y. Shi, T. Bie, M. Shao, Y. Yu, Waveguide Schottky photodetector with tunable barrier based on Ti3C2Tx/p-Si van der Waals heterojunction, Nanophotonics 10 (2021) 4133–4139, https://doi.org/10.1515/nanoph-2021-0415.
[60] S. Wageh, A. Karabulut, A. Dere, A.G. Al-Sehemi, A.A. Al-Ghamdi, F. El-Tantawy, F. Yakuphanoglu, Photodiode based on Pb0.9Cd0.1S ternary alloy semiconductor for solar tracking systems, J. Mater. Sci. Mater. Electron. 29 (2018) 16880–16893, https://doi.org/10.1007/s10854-018-9783-8.
[61] A. Mekki, R.O. Ocaya, A. Dere, A.A. Al-Ghamdi, K. Harrabi, F. Yakuphanoglu, New photodiodes based graphene-organic semiconductor hybrid materials, Synth. Met. 213 (2016) 47–56, https://doi.org/10.1016/j.synthmet.2015.12.026.